Plant, Cell & Environment

Plant, Cell and Environment (2016) **39**, 2725–2739 doi: 10.1111/pce.12828

Original Article

Petunia hybrida PDR2 is involved in herbivore defense by controlling steroidal contents in trichomes

Joëlle Sasse[1], Markus Schlegel[1†], Lorenzo Borghi[1†], Friederike Ullrich[3], Miyoung Lee[1], Guo-Wei Liu[1], José-Luis Giner[4], Oliver Kayser[3], Laurent Bigler[2], Enrico Martinoia[1] & Tobias Kretzschmar[1,5]

[1]*Institute of Plant Biology, University of Zurich, Zurich, Switzerland,* [2]*Department of Chemistry, University of Zurich, Zürich 8008, Switzerland,* [3]*Department of Biochemical and Chemical Engineering, TU Dortmund, Dortmund, Germany,* [4]*Department of Chemistry, SUNY-ESF, Syracuse, NY, USA and* [5]*International Rice Research Institute, Metro Manila, Philippines*

ABSTRACT

As a first line of defense against insect herbivores many plants store high concentrations of toxic and deterrent secondary metabolites in glandular trichomes. Plant Pleiotropic Drug Resistance (PDR)-type ABC transporters are known secondary metabolite transporters, and several have been implicated in pathogen or herbivore defense. Here, we report on *Petunia hybrida* PhPDR2 as a major contributor to trichome-related chemical defense. PhPDR2 was found to localize to the plasma membrane and be predominantly expressed in multicellular glandular trichomes of leaves and stems. Down-regulation of *PhPDR2* via RNA interference (*pdr2*) resulted in a markedly higher susceptibility of the transgenic plants to the generalist foliage feeder *Spodoptera littoralis*. Untargeted screening of *pdr2* trichome metabolite contents showed a significant decrease in petuniasterone and petuniolide content, compounds, which had previously been shown to act as potent toxins against various insects. Our findings suggest that PhPDR2 plays a leading role in controlling petuniasterone levels in leaves and trichomes of petunia, thus contributing to herbivory resistance.

Key-words: Petunia; ABC transporter; glandular trichome; herbivory; metabolomics; secondary metabolism.

INTRODUCTION

Over a million insect species are estimated to feed on terrestrial plants (Howe & Jander 2008), and insect pests have been causing crop losses since the dawn of agriculture (Oerke 2005). Through 400 million years of co-evolution plants developed a number of constitutive and inducible defense responses to cope with insect herbivory. Wax depositions on plant surfaces, foliar defense compounds and leaf hairs (trichomes) are examples for constitutive defenses against biotic stressors (Howe & Jander 2008). Examples of inducible responses include the production of protease inhibitors that impede digestion, the release of volatiles that attract specific predators and the synthesis and activation of toxins (Bodenhausen & Reymond 2007). Toxins and deterrents are often produced and stored in trichomes (Howe & Jander 2008; Bleeker *et al.* 2012; Kang *et al.* 2010b).

Trichomes are uni- or multicellular epidermal protrusions that are formed on aerial parts of plants (Wagner 1991) and are broadly classified into being either non-glandular or glandular. Glandular trichomes consist of a bulbous head on top of stalk cells (Wagner 1991), which is loaded with secondary metabolites. The head is separated from the environment by a cuticule layer only, which bursts easily on contact with an herbivore to release its contents (Wagner 1991). Glandular trichomes are of demonstrated importance in herbivory defense as exemplified by *Datura wrightii*, a species with trichome bimorphism. The variety producing glandular trichomes was observed to be more resistant to herbivory than the variety that produces exclusively non-glandular trichomes (van Dam & Hare 1998; Hare 2005). Glandular trichomes are highly specialized on the production and storage of secondary metabolites, which can make up to 10–15% of the leaf dry weight (Wagner *et al.* 2004).

A plethora of secondary metabolites, among them multiple alkaloids, terpenes, polyketides and phenolics, are believed to have evolved primarily as means of defense and many of them are trichome specific (Wang *et al.* 2001; Yazaki 2006; Schilmiller *et al.* 2008; Slocombe *et al.* 2008; Loreto *et al.* 2014; Kang *et al.* 2010b). Terpenes constitute the largest group of secondary metabolites with over 25 000 known structures that include toxins and deterrents against bacteria, fungi and animals (Gershenzon & Dudareva 2007). Terpenoid metabolism is highly active in glandular trichomes of many species including Solanaceae (Besser *et al.* 2009; Bleeker *et al.* 2012; Tissier *et al.* 2013). Cembranoids, a group of diterpenes in a tobacco variety, were shown to accumulate to approximately 10% of leaf dry weight and 60% of the trichome exudate weight (Wang *et al.* 2001; Wang & Wagner 2003).

Many secondary metabolites are potentially harmful to the plant itself (Cutler *et al.* 1977; Howe & Jander 2008), and thus, plants have developed strategies to avoid autointoxication. Some highly toxic compounds are only fully synthesized upon attack or stored as conjugated inert molecules until activated

Correspondence: L. Bigler, E. Martinoia and T. Kretzschmar. e-mail: laurent.bigler@chem.uzh.ch; Enrico.Martinoia@botinst.uzh.ch; t.kretzschmar@irri.org

[†]*equally contributing second authors*

upon tissue wounding. Many defense compounds are either stored within vacuoles or secreted into the apoplast, places that are not connected to the plant's primary metabolism. On tissue level, they are stored in specialized organs such as glandular trichomes, laticifers or secretory ducts. Indeed, apart from import of energy-rich compounds and precursors for specialized biosynthetic pathways, trichome metabolism is largely disconnected from the rest of the plant metabolism (Schilmiller *et al.* 2008). However, many compounds, such as terpenoids, are hydrophobic and tend to diffuse across membranes along their concentration gradient. To avoid toxic effects because of reflux, steep concentration gradients have to be maintained between sites of synthesis and storage that likely depend on the existence of energy-dependent transporters.

Transporters that directly utilize adenosine triphosphate (ATP) as an energy source are more efficient in establishing and maintaining steep concentration gradients than those relying on electrochemical gradients (Kreuz *et al.* 1996) Thus, proteins of the ATP binding cassette (ABC) family (Yazaki 2006; Kang *et al.* 2011) are primary candidates to create and maintain the postulated strong gradients between trichomes and leaves or trichome heads and stalk cells. ABC proteins are present in all kingdoms, from bacteria to humans (Theodoulou 2000), but they are most abundant and diversified in plants. ABC members of the ABCG subfamily have been reported to be involved in lipid and phytohormone transport, biotic stress responses of plants and in transport of secondary metabolites (Kang *et al.* 2011; Kretzschmar *et al.* 2012; Banasiak *et al.* 2013; Hwang *et al.* 2016). Many full-size ABCG members, also termed Pleiotropic Drug Resistance (PDR) proteins, are transcriptionally responsive to pathogen elicitors and jasmonic acid (JA) treatment (Kretzschmar *et al.* 2011). NtPDR1 and NpPDR1 were furthermore demonstrated to be expressed in glandular trichomes (Sasabe *et al.* 2002; Stukkens *et al.* 2005; Crouzet *et al.* 2013) and involved in transport of the fungi-toxic diterpene sclareol (Cutler *et al.* 1977; Jasinski *et al.* 2001; Crouzet *et al.* 2013). NtPDR5 was described as responsive to herbivory, its expression being induced upon JA treatment, mechanical wounding and feeding by the Solanaceae specialist *Manduca sexta* (Bienert *et al.* 2012). However, potential substrates of this transporter remain unknown.

Collectively, PDR proteins are plasma membrane intrinsic secondary metabolite transporters that have been found in trichomes, making them excellent candidates for cellular export of deterrents and toxins related to herbivory. We performed our analysis in petunia, which serves as a Solanaceae model species (Gerats & Vandenbussche 2005) and has leaves that are highly toxic to herbivores. Here, we report on PhPDR2, which localizes to glandular trichomes of petunia leaf and stem tissue and is involved in herbivore defense presumably through modulation of insecticidal steroidal compounds.

METHODS

Plant growth conditions

All experiments were performed with *Petunia hybrida* cultivar W115. Plants were grown under long day conditions with 16 h of continuous light at 40% relative humidity. Plants were either grown on soil (ED 73 Einheitserde) or on clay granules (Oil Dry US Special from Damolin) supplemented once a week with 1× Hoagland solution. On plate, plants were grown on medium containing 2.2 g L^{-1} MS (Duchefa) and with or without 15 g L^{-1} sucrose (0.5 MS – Suc, 0.5 MS + Suc plates, respectively), supplemented with 9 g L^{-1} phyto agar (Duchefa) at 16 h of light and 25 °C.

Conserved *PDR* domain amplification

For the investigation of petunia *PDR* sequences expressed in leaf and trichome tissue, primers were designed on a CDS alignment of *PDRs* from different Solanaceae. *Solanum lycopersicum* sequences were obtained from a Blast of *PhPDR2* and *PDR1* against the tomato database (http://mips.helmholtz-muenchen.de/plant/tomato/database). The search resulted in 23 hits listed in the Accession Numbers section. *Solanum tuberosum* CDS were obtained from GenBank for *StPDR1 – StPDR4*, and by a Blast search with *PDR1* and *PhPDR2* against the *S. tuberosum* database (http://solgenomics.net/organism/Solanum_tuberosum/genome), which resulted in 29 hits listed in the Accession Numbers section. Furthermore, the *Nicotiana plumbaginifolia* CDS of *NpPDR1*, *NpPDR2*, *NpPDR3*, *NpPDR5*, the *Nicotiana tabacum NtPDR1*, *NtPDR3*, *NtPDR4*, *NtPDR5a* and *NtPDR5b* were included. The Walker A box of NBD 2 and the PDR signature 4 were part of the most conserved part of the alignment. Thus, PCR was performed on this region (F 5′-agcwytrrtgggwgtyagtggdgctgg, R 5′-ctcatcaaadgcttcaaawatgtc), and the fragments were cloned into pGEM®-T easy vector (Promega, USA), sequenced and aligned with the MultAlin software (http://multalin.toulouse.inra.fr/multalin/). Fragments that were only amplified once were excluded from the analysis.

PhPDR2 phylogenetic analysis

To set PhPDR2 in relation to described PDR proteins, the well-established *Oryza sativa* and the *Arabidopsis thaliana* PDR proteins, as well as *Spirodela polyrrhiza SpTUR2*, *Glycine max GmPDR12*, the *Nicotiana plumbaginifola NpPDR1*, *NpPDR2*, *NpPDR3*, *NpPDR5*, the *N. tabacum NtPDR1*, *NtPDR3*, *NtPDR4*, *NtPDR5a*, *NtPDR5b* and the *P. hybrida* PDR1 were included in the analysis. PDR Clusters were annotated after Crouzet *et al.* 2006. The conserved region (see Conserved domain analysis) of the respective genes was identified and phylogeny of the 0.5 kb fragments was analyzed with a maximum-likelihood tree created on Phylogeny.fr (http://www.phylogeny.fr/)(Dereeper *et al.* 2008) with the following settings: 16 maximal iterations in MUSCLE alignment, minimal block length of 10 and no gap positions in Gblocks 0.91b alignment refinement (Dereeper *et al.* 2008).

PhPDR2 transcriptional induction and quantitative PCR

For hormone and elicitor treatment 14-day-old W115 seedlings grown on plate were exposed for 24 h with final concentrations of 100 μM salicylic acid (SA), 0.1 mL L^{-1} methyl-jasmonate (MJa), 10 g L^{-1} yeast extract, 10 μM abscisic acid (ABA), 25 μM 1-naphthaleneacetic acid (NAA) or 500 μM sclareol.

RNA was isolated with the RNeasy Plant Mini Kit (Qiagen USA) and reverse transcribed to cDNA with M-MLV Reverse Transcriptase (Promega, USA). Quantitative PCR was performed with 5′-TCAAGGCATTCAACTTCCAG and 5′-TACTGACCGAGTCTCCACCA for *PhPDR2* transcription level detection in seedlings and in various tissues. Glyceraldehyde-3-phosphate dehydrogenase (GapDH) served as a housekeeping gene and was amplified with 5′-GACTGGAGAGGTGGAAGAGC and 5′-CCGTTAAGAGCTGGGAGAAC. All reactions were performed in SYBR Green PCR Master Mix (Applied Biosystems) on a 7500 Fast Real-Time PCR system (Applied Biosystems).

PhPDR2 cloning strategy

Partial sequences of putative ABCG/*PDR* transcripts were amplified from total cDNA of W115 individuals. NBD1-specific amplicons of around 0.5 kb were obtained with 5′-mgwatgactctdytkytkggacctcc targeting PDR signature 1 and 5′-gyttcytytgncchcchgaaatwcc targeting the ABC signature. NBD2-specific amplicons of around 0.5 kb were obtained with 5′-gggwaaracggwgtyagtggwgcw targeting the Walker A box and 5′-ctcatnacaatdgcwgcwgctctwgc targeting PDR signature 3. Fragments for the respective NBDs were aligned, and the *ABCG/PDR* subfamily specific consensus primers (F 5′-tattgggacttgaaatttgtgccgatac, R 5′-gctccactaacacccatcagagctgtc) were designed to amplify putative *ABCG/PDR* coding regions spanning NBD1 and NBD2 from W115 trichome cDNA.

Amplification of upstream and downstream sequences of *PhPDR2* full length transcript was achieved via 5′RACE and 3′RACE PCRs using the SMART-RACE cDNA Amplification Kit (Clontech, Takara Bio Company, USA) according to the manufacturers' specifications. 5′ RACE primer and 5′ nested RACE primer had the following sequence: 5′-atggattcgaagaaggccagaacgtcttc and 5′-cccttaccatgtcatctcccaccaaag. 3′ RACE primer and nested 3′ RACE primer sequences were: 5′-gatcagggtgcctctgaagatagattgg and 5′-caggaggatatattgagggtagaatccaca.

The *PhPDR2* genomic DNA sequence was cloned in two sequential steps from W115 DNA. Firstly, a 2.6 kb 5′ part was amplified (F 5′-atcccgggataatggaaccagtaaac, R 5′-ttaaggatccggatcccgtcatgtgaccaa, F contains a *Xma*I site and R a endogenous *Bam*HI site (underlined)). The PCR product was T/A cloned into pGEM®-T easy (Promega). Secondly, the 3′ 5.3 kb part of *PhPDR2* was amplified in to single PCRs. PCR1: F1 5′-ttaaggatccttggtcacatgacgggatcc with the endogenous *Bam*HI site (underlined), R1 5′-catcatcggtgaagtccagt. PCR2: F2 5′-gaagaaatggtggat, R2 5′-taagcggccgcctatcttgtctggaagtt with a *Not*I site (underlined). A second PCR (F1 and R2) resulted in amplification of the full 5.3 kb. The PCR product was cloned into pGEM®-T easy (Promega). Both genomic fragments were transferred into the binary pGreenII0229 vector system (Hellens *et al.* 2000). A *CaMV 35S* promoter was added with 5′-gggcccgtcaaagattcaaatagaggac and 5′-ctcgagtgtcctctccaaatgaaatg containing an *Apa*I and *Xho*I restriction site, respectively (underlined), a N-terminal *GFP5* was added with 5′-gtcgacatgagtaaaggagaagaac and 5′-ctgcagatctttcgaaagggcagatt containing a *Sal*I and *Pst*I restriction site, respectively (underlined), and an *OCE3* terminator was added with 5′-agcggccgcaatttccccgatcgttca and 5′-gcggccgccgatctagtaacatagatga containing *Not*I restriction sites (underlined).

PhPDR2 promoter GUS constructs and GUS staining assay

Amplification of a 1.2 kb promoter fragment upstream of the *PhPDR2* gene was accomplished via use of the Genome Walker Universal Kit (Clontech, Takara Bio Company, USA) with the primer 5′-caagagctgcccatttaagtgcttcttc and the nested primer 5′-cgcttaaacttccccttgcacttcctc. The fragment was T/A cloned into pGEM-T Easy vector system (Promega, USA) and subsequently reamplified with the primer 5′-ggaaccaagctttgtgtaggaaaattttgc containing a *Hind*III restriction site (underlined) and the primer 5′-tacatctagagaccccctctagctcag containing an *Xba*I restriction site (underlined). The respective restriction sites were used to clone the *PhPDR2* promoter fragment into the *GUS* gene-containing pGPTV-Bar (Becker *et al.* 1992) vector system.

For GUS staining trials tissues to be investigated were submerged in an appropriate amount of GUS-staining buffer (100 mM sodium phosphate buffer pH 7.0, 10 mM NaEDTA, 1.5 mM potassium hexacyanoferrate(II) trihydrate, 0.25 mM potassium hexacyanoferrate(III), 0.1% (v/v) Triton X-100 and 1 mM 5-bromo-4-chloro-3-indolyl β-D-glucuronide cyclohexylammonium salt) vacuum infiltrated three times for 30 s and incubated in the dark at 37 °C for 12 – 24 h. After staining samples were cleared and stored in 70% ethanol.

PhPDR2 RNA interference constructs

Silencing of *PhPDR2* specific transcripts was attempted via the generation of double stranded hairpin RNA fragments utilizing the pKANIBAL vector system (Wesley *et al.* 2001). A 407 bp fragment containing parts of the 3′ end and the 3′ UTR of *PhPDR2* was amplified from *PhPDR2* cDNA with 5′-cgatggatcctcgagctgatgatgaaacagtggaa, containing *BamH*I and *Xho*I restriction sites (underlined) and 5′-cgatatcgatggtaccgaataaatatgccgctttca containing *Cla*I and *Kpn*I sites (underlined). The resulting amplicon was cloned in sense and antisense direction in the two MCS of pKANIBAL flanking the hairpin intron sequence. The pKANIBAL RNAi cassette containing *CaMV 35S* promoter RNAi construct and *OCE3* terminator was excised from the vector backbone using the *Not*I restriction sites and transferred into the binary pGreenII0229 vector system (Hellens *et al.* 2000),

conferring Glufosinate Ammonium resistance as a selection marker in plants.

After stable transformation of W115 plants, the degree of down-regulation in several independent *PhPDR2* lines was estimated via semi-quantitative RT-PCR using the *PhPDR2* specific primers 5′-ggaatgtattctgccttacc and 5′-gtaatctccaaattgtgatgc. Petunia tubulin 1 transcript, partially amplified with 5′-cattggtcaagccggttattc and 5′-acccttgaagaccagtacagt, served as a housekeeping and loading control.

Transient *Arabidopsis thaliana* transformation

A. thaliana Col-0 plants were grown in a 8 h light, 16 h dark cycle at 21 °C at 60% relative humidity. Leaves of 2-month-old plants were collected, the abaxial cuticule removed with sand paper and digested at 23 °C, gentle shaking, for 1.5 h in 0.4 M mannitol, 20 mM KCl, 20 mM MES, 0.4% [w/v] macerozyme R10 (Yakult Honsha, Japan), 1% [w/v] cellulase R10 (Yakult Honsha, Japan), pH 5.7. After the digestion, 10 mM $CaCl_2$ was added, and protoplasts were collected at 400 *g* for 5 min at 4 °C with low break. Supernatant was removed, and the pellet was solubilized in W5 solution (154 mM NaCl, 125 mM $CaCl_2$, 5 mM KCl, 2 mM MES, pH 5.7) and the pellet was moved to a tube containing 21% [w/v] sucrose. The protoplasts were collected at 400 *g* for 6 min at 4 °C with low break, the supernatant removed, and cells were transferred to a new tube. W5 solution was added, and the protoplasts were incubated 30 min on ice and collected at 400 *g* for 3 min at 4 °C with low break. Protoplasts were collected, and density was adjusted to 2×10^5 cells mL^{-1} in MMg solution (0.4 M mannitol, 15 mM $MgCl_2$, 4 mM MES pH 5.7).

The pGreen179 plasmid containing the 35S:GFP-PDR2 construct was purified with the Plasmid Plus Midi Kit (Qiagen); 10 μg of the construct and 10 μg of the plasma membrane marker *AtAHA2-RFP* (Lee *et al.* 2003) were added to the protoplasts, as well as 220 μL of PEG solution (40% [w/v] PEG 4000, 0.2 M mannitol, 0.1 M $CaCl_2$). Protoplasts were incubated for 5 min at 23 °C. Further, 800 μL of W5 solution was added, and cells were collected 400 *g* for 3 min at 4 °C with low break. The supernatant was removed fully, and 100 μL of W5 solution was added. Protoplasts were incubated in the dark for 2 d at 23 °C.

Stable petunia transformation

PhPDR2 promoter GUS constructs and *PhPDR2* RNAi constructs were transferred into the W115 background via *Agrobacterium tumefaciens* mediated transformation of leaf explants, callus induction and plant regeneration (Lutke 2006); 0.45% phytagel were used instead of 0.9% agar in all media, and the concentrations of BAP and NAA in the Selection Medium were adjusted between 1 and 2 mg L^{-1} for the former and 0.05 and 0.15 mg L^{-1} for the latter to maximize shoot induction for each individual transformation.

Regenerated plantlets were tested for successful construct insertion via PCR on genomic DNA. The primers 5′-acggtccacatgccggtatatacgatg and 5′-gatggcatttgtaggagccaccttcc, targeting the *CaMV 35S* promoter, were used to confirm RNAi construct insertion. The primers 5′-gaattgatcagcgttggtgggaaagc and 5′-ggtaatgcgaggtacggtaggagttg, targeting the GUS gene, were used to confirm GUS construct insertion.

Trichome quantification

Leaves of 3-month-old, greenhouse-grown W115 plants ($n = 6$) were quantified for trichome density; 0.5 cm^2 leaf fragments were collected at the middle leaf margin and on the middle leaf lamina. Each leaf fragment was then cut into five 0.5×0.1 cm strips for trichome quantification on both adaxial and abaxial sides at the stereomicroscope.

Sclareol growth assays

For the germination assay, seeds of wild type and *PhPDR2*-RNAi lines were grown on 0.5 MS – Suc plates supplemented with 0, 100, 250 or 500 μM sclareol. The germination rate was determined after xx days. For the root growth assay, wild type and *PhPDR2*-RNAi lines were grown on 0.5 MS – Suc plates for xx days, after which the plantlets were transferred to 0.5 MS – Suc plates supplemented with 0, 100, 250 or 500 μM sclareol. Primary root length was determined for plants grown on sclareol containing plates after xx days and expressed relative to plants grown on plates not supplemented with sclareol. *PhPDR2* promoter GUS reporter containing lines were grown and stained as described above.

Spodoptera littoralis feeding trials

All larvae for the leaf feeding experiments were kindly provided by Syngenta, Switzerland. Second instar *S. littoralis* larvae were placed in ventilated transparent plastic containers ($10 \times 10.5 \times 4.5$ cm). The bottom was covered with a moist paper towel, and every 1–2 days larvae were supplied with fresh leaves. It was taken care, that their position and developmental stage were the same. The uppermost fully expanded leaves were taken for feeding trials. To ensure that excised leaves kept their turgor, cut petioles ends were inserted into small water containers and sealed with parafilm. All larvae were weighted in regular intervals, and their mortality was recorded. A linear model using generalized least squares of the nlme package for the R software (R Development Core Team, 2009, version 2.9.2) was utilized for comparing weight of larvae at different time points. W115 data was set as intercept of the model.

Survival probabilities were calculated as Kaplan–Meier curves.

Leaf washes

Leaves of seven 3-month-old, greenhouse-grown W115, *pdr2*[1], *phdr2*[2] and *pdr2*[3] plants were incubated with the adaxial surface in a glass petri dish with 8 mL of isopropanol:acetonitrile: water 3:3:2 solution for 5 min at 23 °C with gentle shaking. The solution was collected and stored at −20 °C for further use. Samples were concentrated using Oasis HLB 6 cc

extraction cartridges (Waters). The cartridges were conditioned with methanol, equilibrated with water and loaded with the samples. After washing with 5 mL water, the cartridges were eluted with 6 mL methanol. Samples were dried under N_2 and resuspended in 200 μL of a isopropanol:acetonitrile:water solution (Kang *et al.* 2010a) containing two internal standards, 0.05% (+) camphor-10-sulfonic acid (purum, Fluka, Germany) and 0.05% lidocaine hydrochloride monohydrate (Sigma, Germany). Samples were suspended in an ultrasonic bath for 1 min, centrifuged at 13 000 *g* at 4 °C for 5 min; 5 μL of the supernatant were used for ultra-high performance liquid chromatography (UHPLC) coupled with high-resolution mass spectrometry (HR-MS).

UHPLC-HR-ESI-MS and MS/MS analyses

Samples were analyzed with an ultra-high performance (UHPLC) high-resolution mass spectrometry (HR-MS), which was composed of a Waters Acquity UPLC system (Waters, USA) connected to a maXis quadrupole time-of-flight MS (Bruker Daltonics, Germany). Plant metabolites were separated at 40 °C on a Waters Acquity UPLC BEH column (1 × 50 mm, 1.7 μm) with a flow rate of 0.2 mL min^{-1}, and a mobile phase composed of water (solution A) and acetonitrile (solution B), both of which containing 0.1% HCOOH. The gradient program conditions were: 3% of solvent B during 0.5 min followed by a linear gradient up to 99.5% within 8 min. The gradient was followed by a washing step with 99.5% solvent B for 2.5 min and a re-equilibration step to the initial composition for 2 min. The UHPLC was connected to the MS equipped with an electrospray ion source (ESI) operated either in positive (+) or in negative (−) ionization mode. Nitrogen was used as nebulizer (2.0 bar) and as dry gas (9 L min^{-1}, 205 °C) and as collision gas. MS acquisitions were performed in the mass range from *m/z* 50 to 1500 at 20 000 resolution (full width at half maximum) and 1.5 scan s^{-1}. Masses were calibrated below 2 µg g^{-1} accuracy with a 2 mM solution of sodium formate over *m/z* 158 up to 1450 mass range prior analysis. MS/MS data consisted of averaged spectra acquired at 15, 20 and 30 eV collision energy, at 4 Hz scan rate, in the mass range *m/z* 50 to 800, and with N_2 as collision gas. Relative metabolite amounts were obtained by manual integration of corresponding signals found in theoretical extracted ion chromatograms (EIC) with ±0.05 Da width.

The Bruker ProfileAnalysis™ application (Version 2.1, Bruker Daltonics, Germany) was used for unsupervised principal component analysis (PCA) processing of the HR-ESI-MS data. Conspicuous masses having more than 50% reduction of signal intensity in *PhPDR2* lines compared to W115 were selected. The corresponding molecular formulas of these masses were calculated at 2 µg g^{-1} mass accuracy with Smart Formula®, part of the DataAnalysis™ processing software (Bruker Daltonics, Germany). Metabolites of interest for *Petunia sp.* were finally identified with SciFinder® database (www.cas.org, American Chemical Society) and literature data (Elliger *et al.* 1988a,1988b; Elliger *et al.* 1989a; Elliger *et al.* 1990a,1990b; Elliger & Waiss 1991; Elliger *et al.* 1992; Elliger *et al.* 1993; Tarling *et al.* 2013).

The UHPLC-HR-ESI-MS data was in addition processed with XCMS Online (http://metlin.scripps.edu/xcms/, Metlin (Tautenhahn *et al.* 2012)) analyzing all *pdr2* lines versus W115. Following parameters were selected: centwave detection method, 10 µg g^{-1} mass accuracy, 5 < UHPLC peak width < 20, obiwarp retention time correction, unpaired parametric *t*-test (Welch *t*-test, unequal variances), 0.001 statistical threshold. Masses of the aforementioned petuniasterols and petuniolides were identified in the XCMS results file. The flavonoids were detected in negative ionization mode.

Relative petuniolide and petuniasterone amounts in leaves

Leaf margin (ca. 3 mm from the edge) and inner side of the leaves were collected by cutting 3-month-old W115 plants (6 replicates) and two *pdr2*^{1}, *phdr2*^{2} and *pdr2*^{3} plants each, and stored at −80 °C before extraction.

The leaves were immerged in liquid air, grinded manually at temperatures below −10 °C. To 50 mg of the frozen sample, 1 mL of the precooled (−18 °C) extraction mixture 1 (methanol containing 2 µg mL^{-1} corticosterone (ISTD)/methyl tert-butyl methylether (MTBE) 1:4) was added, shaken, incubated 10 min on ice and sonicated for 10 min at 0 °C. Then, 500 μL of extraction mixture 2 (water/methanol 3:1) was added at 23 °C. Following vortexing and centrifugation (2 min, 13 000 *g*), aliquots of the upper phases (600 μL) were transferred to new tubes, and the solvent was evaporated with N_2 gas at 23 °C. Finally, the samples were re-suspended in 200 μL of acetonitrile/isopropanol 7:3 and used for UHPLC-MS analysis.

Samples (1 μL injection) were analyzed with UHPLC-HR-MS instrumentation described above in a random sequence. Chromatographic conditions were different: separation at 60 °C on a Waters Acquity UPLC BEH C8 column (2.1 × 100 mm, 1.7 μm) with a flow rate of 0.4 mL min^{-1}, and a mobile phase composed of water (solution A) and acetonitrile (solution B), both them containing 1% of 1 M aq. NH_4OAc and 0.1% AcOH. Elution was started with 5% of solvent B during 1 min followed by a linear gradient up to 100% within 12 min. The gradient was followed by a washing step with 100% solvent B for 5 min and a re-equilibration step to the initial composition for 4 min. Data were quantitatively processed with the *Bruker Data Analysis* software by manual integration of the high-resolution extracted ion chromatograms (width of ±0.01 Da) corresponding to the calculated exact masses of the following detected ionized molecules (EIC of the ionized species were combined to improve sensitivity) (Supplemental Table 3).

The peak areas shown in Fig. 7 were normalized to 50 mg leaf material and to the ISTD according to following equation:

$$Area_{corr}[AU] = area_{compound} \times \frac{mass_{leaf}}{50\ mg} \times \frac{average(areas_{ISTD})}{area_{ISTD}}.$$

Statistical analyses

Data were analyzed using the R software (R Development Core Team 2009), version 2.9.2. For comparing the weight (resp. weight gain) of larvae on wildtype versus *pdr2* plants, a linear model using generalized least squares (gls) was applied from the package *nlme*. W115 data were set to represent the intercept of the model, against which each line is compared. From survival data, Kaplan–Meier estimates were calculated using the *survival* package in R, and *pdr2* survival curves were then tested for significant differences compared to the W115 curve. For all statistical analyzes, significance was reported at the level $\alpha = 0.05$.

Accession numbers

Sequence data from this article can be found in the GenBank data library, the tomato genome database (http://mips.helmholtz-muenchen.de/plant/tomato/database) and the potato genome of Solgenomics network (http://solgenomics.net/organism/Solanum_tuberosum/genome) in under the following accession numbers:*Arabidopsis thaliana*At-*PDR1/ABCG29/*At3g16340 (BK001001), At-*PDR2/ABCG30/*At4g15230 (BK001000), At-*PDR3/ABCG31/*At2g29940 (BK001002), At-*PDR4/ABCG32/*At2g26910 (BK001003), At-*PDR5/ABCG33*/At2g37280 (BK001004), At-*PDR6/ABCG34/*At2g36380 (BK001005), At-*PDR7/ABCG35/*At1g15210 (BK001006), At-*PDR8/ABCG36/*At1g59870 (BK001007), At-*PDR9/ABCG37*/At3g53480 (BK001008), At-*PDR10/ABCG38*/At3g30842 (BK001009), At-*PDR11/ABCG39*/At1g66950(BK001010), At-*PDR12/ABCG40/*At1g15520 (BK001011), At-*PDR13/ABCG41*/At4g15215 (BK001012), At-*PDR14/ABCG42/*At4g15233 (BK001013), At-*PDR15/ABCG43*/At4g15236 (BK001014)*Glycine max*Gm-*PDR12* (Q1M2R7)*Nicotiana plumbaginifolia*Np-*PDR1* (AJ404328.1), Np-*PDR2* (AJ831424.1), Np-*PDR3* (AJ831379.1), Np-*PDR5* (JQ808000.1)*Nicotiana tabacum*Nt-*PDR1* (AB075550.1), Nt-*PDR3* (AJ831379.1), Nt-*PDR4* (AJ831380.1), Nt-*PDR5a* (JQ808002.1), Nt-*PDR5b* (JQ808003.1)*Oryza sativa*Os-*PDR1* (BK001015), Os-*PDR2* (BK001016), Os-*PDR3* (BK001017), Os-*PDR4* (BK001018), Os-*PDR5* (AJ535050), Os-*PDR6* (AJ535049), Os-*PDR7* (AJ535048), Os-*PDR8* (AJ535047), Os-*PDR9* (AJ535046), Os-*PDR10* (AJ535045), Os-*PDR11* (AJ535044), Os-*PDR12* (AJ535043), Os-*PDR13* (AJ535042), Os-*PDR15* (AJ535041), Os-*PDR16* (AAQ01165.1), Os-*PDR17* (AK100858), Os-*PDR18* (AK072827), Os-*PDR20* (EAZ44307.1), Os-*PDR21* (AK070409), Os-*PDR22* (AK107869), Os-*PDR23*_1 (AK102367), Os-*PDR23*_2 (AK103110)*Petunia hybrida*Ph-*PDR1* (JQ292813), Ph-*PDR2* (KU665392)*Solanum lycopersicum*Solyc02g081870.2.1, Solyc06g076930.1.1, Solyc05g018510.2.1, Solyc11g007300.1.1, Solyc06g036240.1.1, Solyc12g098210.1.1, Solyc09g091660.2.1, Solyc12g100190.1.1, Solyc12g100180.1.1, Solyc12g019640.1.1, Solyc11g067000.1.1, Solyc11g007290.1.1, Solyc11g007280.1.1, Solyc09g091670.2.1, Solyc08g067620.2.1, Solyc08g067610.2.1, Solyc06g065670.2.1, Solyc05g055330.2.1, Solyc05g053610.2.1, Solyc05g053600.2.1, Solyc05g053590.2.1, Solyc05g053570.2.1, Solyc03g120980.2.1*Solanum tuberosum*St-*PDR1* (JF720054.1), St-*PDR2* (JF440348.1), St-*PDR3* (JF720055.1), St-*PDR4* (JF720056.1) PGSC0003DMC400041247 PGSC0003DMT400061280, PGSC0003DMC400051611 PGSC0003DMT400076208, PGSC0003DMC400023214 PGSC0003DMT400034124, PGSC0003DMC400051609 PGSC0003DMT400076206, PGSC0003DMC400023219 PGSC0003DMT400034130, PGSC0003DMC400051612 PGSC0003DMT400076209, PGSC0003DMC400033296 PGSC0003DMT400049313, PGSC0003DMC400033294 PGSC0003DMT400049311, PGSC0003DMC400029466 PGSC0003DMT400043433, PGSC0003DMC400033295 PGSC0003DMT400049312, PGSC0003DMC400004038 PGSC0003DMT400005783, PGSC0003DMC400004040 PGSC0003DMT400005785, PGSC0003DMC400032813: 1-1200 PGSC0003DMT400048449, PGSC0003DMC400050377 PGSC0003DMT400074382, PGSC0003DMC400050376.*Spirodela polyrrhiza*Sp-*TUR2* (CAA94437)

RESULTS

Screen for *PDR* sequences expressed in leaves and trichomes

To identify petunia secondary metabolite transporters possibly involved in herbivore defense, a screen for PDR transcripts present in leaves and trichomes was performed with degenerate consensus primers targeting a highly conserved region of Solanaceae PDR sequences. Thirty-two cloned and sequenced amplicons of 0.5 kilobase (kb) size could be assigned to four putative genes, *PhPDR2* – *PhPDR5* (Fig. 1). The *PhPDR2* fragment was the most abundant comprising 47% of the analyzed sequences. *PhPDR3* comprised 25% of the amplified sequences, whereas *PDR4* and *PDR5* were lowest in abundance comprising 16% and 12% the sequences, respectively. *PhPDR2* was amplified from trichomes as well as from leaves devoid of trichomes. *PhPDR4* was mainly expressed in trichomes, while *PhPDR3* and *PhPDR5* were mainly found in leaf tissue (Supplemental Figure 1).

A phylogenetic analysis was performed to relate petunia *PhPDR2* – *PhPDR5* fragments to reported PDR sequences of petunia, tomato (*S. lycopersicum*), rice (*O. sativa*), Arabidopsis (*A. thaliana*), *Nicotiana sp*., *S. polyrrhiza*, and soybean (*G. max)* (Supplemental Figure 2). This analysis assigned *PhPDR2*, *PhPDR3* and *PhPDR4* to cluster I of PDR proteins and *PhPDR5* to cluster III (Supplemental Figure 2) (Crouzet *et al.* 2006). An additional phylogenetic analysis with focus on functionally characterized PDR genes (Jasinski *et al.* 2001; Sasabe *et al.* 2002; van den Brule & Smart 2002; Campbell *et al.* 2003; Ducos *et al.* 2005; Lee *et al.* 2005; Eichhorn *et al.* 2006; Ito & Gray 2006; Kobae *et al.* 2006; Kim *et al.* 2007; Badri *et al.* 2008; Galbiati *et al.* 2008; Trombik *et al.* 2008; Bessire *et al.* 2011; Chen *et al.* 2011; Xi *et al.* 2011; Bienert *et al.* 2012; Kretzschmar *et al.* 2012), revealed that all petunia *PDR* fragments, except *PhPDR2*, clustered closely with already characterized *PDR* sequences (Fig. 1). PhPDR3 was found to be highly homologous with NpPDR1, while the trichome-specific PhPDR4 was near identical with NtPDR1. Closest relatives of PhPDR2 were NtPDR1, NpPDR1, AtPDR12 and GmPDR12 (Supplemental Figure 2), with an

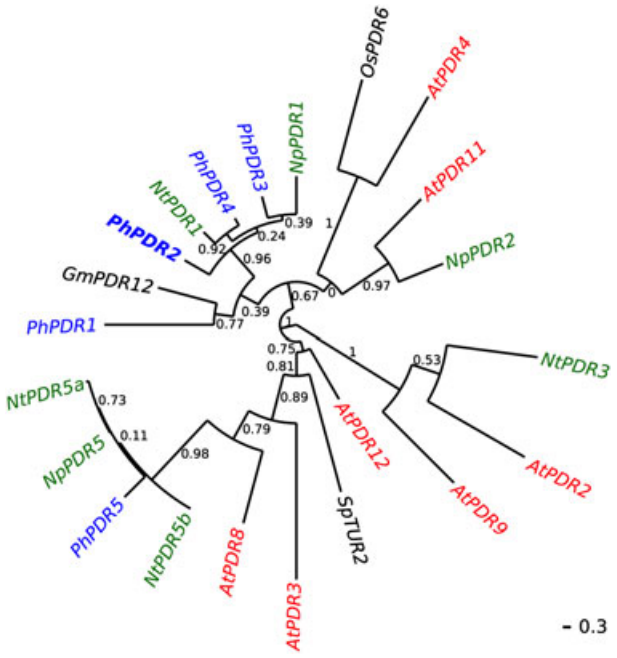

Figure 1. Phylogeny of Ph-*PDR* sequences. Phylogeny of *Petunia hybrida PDR2 – PDR5* fragments (blue) and the respective fragments, identified by sequence similarity, of reported PDR sequences of *Arabidopsis thaliana* (red), *Nicotiana tabacum* and *N. plumbaginifolia* (green), *Spirodela polyrrhiza* (black), rice (black) and *Glycine max* (black).

amino acid identity of 81%, 80%, 69% and 65%, respectively. Because of the distinctiveness of PhPDR2 and its relatively high abundance, we decided to focus further investigations on this sequence. To avoid possible redundancy PhPDR3 and PhPDR4 were dismissed from further analyses as they were likely orthologous with well-characterized NpPDR1 (Jasinski *et al.* 2001; Stukkens *et al.* 2005) and NtPDR1 (Sasabe *et al.* 2002; Crouzet *et al.* 2013), respectively.

The 7541 bp genomic DNA sequence (start ATG to stop TGA) of *PhPDR2* consisted of 20 exons (Supplemental Figure 3a); 265 bp upstream of the start ATG, a putative methyl jasmonate (MJA)-responsive element (AACGTG) (Guerineau *et al.* 2003), was detected. Sequencing of the full length *PhPDR2* cDNA revealed an ORF of 4287 base pairs (bp), an 5′ UTR of 135 bp, 3′UTR of 253 bp followed by a poly-A tail, resulting in a cDNA size of 4701 bp. The predicted polypeptide of 1429 amino acid residues and a molecular mass of ~162 kD featured a reverse organization of the two NBDs and the transmembrane domains (TMDs), distinct for full size ABCG type transporters (Supplemental Figure 3b). The *PhPDR2* NBDs contain the ATP-binding Walker A and B motifs (Walker *et al.* 1982), the ABC signatures (Martinoia *et al.* 2002) and all four PDR signatures (van den Brule & Smart 2002).

PhPDR2 subcellular localization and expression pattern

PDR proteins characterized to date localized exclusively to the plasma membrane. For localization of PhPDR2, its genomic sequence was fused to a green fluorescent protein (GFP) reporter sequence (*P35S:GFP-gPDR2*). *At-AHA2*, fused to a red fluorescent protein (*P35S:cAHA2-RFP*), served as a marker for plasma membrane localization (Lee *et al.* 2003). *A. thaliana* mesophyll protoplasts were transiently co-transformed with the aforementioned constructs, and fluorescent signals were recorded. The overlay of the GFP and RFP signals revealed co-localization of the two recombinant proteins (Fig. 2), indicating that PhPDR2 localized to the plasma membrane.

To investigate whether *PhPDR2* was expressed in tissues other than trichomes and leaves, quantitative RT-PCR was performed on RNA extracted from 14-day-old seedlings, from two-month-old roots and stems, from flower tissue and from selected leaf regions, and the values were expressed relative to expression in full leaf samples. *PhPDR2* transcripts were detected in low amounts in flowers, to a higher degree in whole seedlings, roots and stems, and in highest amounts in leaf samples (Fig. 3a). *PhPDR2* expression was higher in leaf borders than in the central part of the leaf. Leaves devoid of trichomes showed lower expression of *PhPDR2* than full leaf samples, and transcription of *PhPDR2* was significantly enriched in pure leaf trichome samples (Fig. 3a).

In order to obtain a more detailed picture of *PhPDR2* expression on a tissue specific level, a 1.2 kb genomic fragment upstream of the *PhPDR2* coding sequence was fused with the GUS reporter gene and stably transformed into the petunia cultivar W115. In foliar tissue, *PhPDR2* promoter activity was found around the leaf margins (Fig. 4a) and in multicellular glandular trichomes (Fig. 4b–c), including the epidermal cells

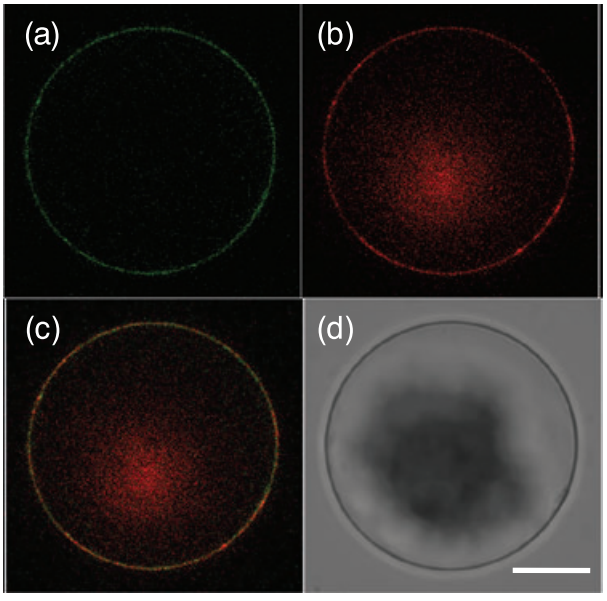

Figure 2. PDR2 localizes to the plasma membrane. *Arabidopsis thaliana* mesophyll protoplasts were transiently co-transformed with a 35S::*GFP-PDR2* construct and the plasma membrane marker AHA2-RFP. (a) PDR2 GFP signal, (b) AHA2 RFP signal, (c) overlay of (a) and (b), (d), bright field image of the same cell shown in (a–c). Scale bar: 10 μm.

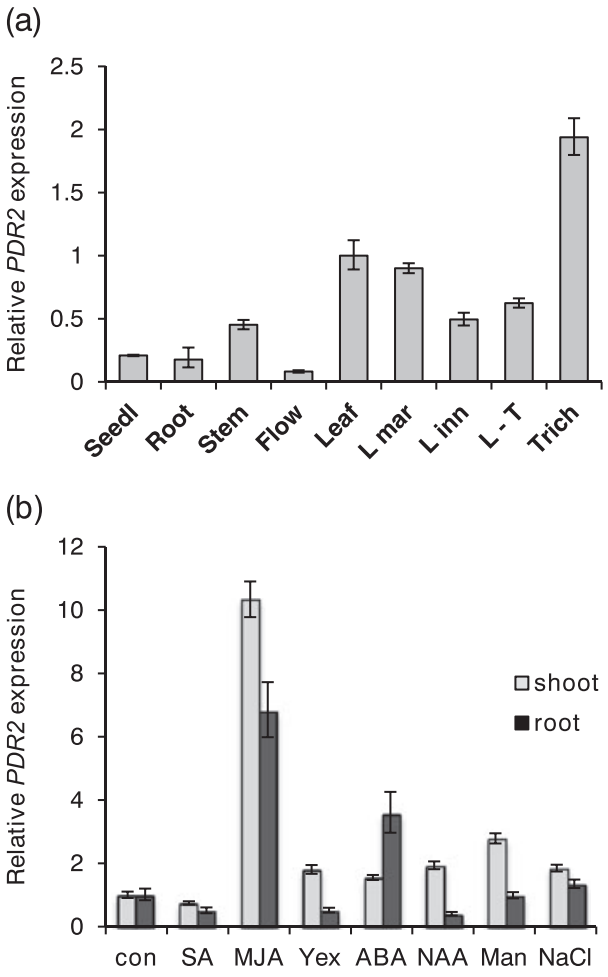

Figure 3. *PDR2* is expressed in leaf and stem trichomes, and it is induced by jasmonic acid. (a) Quantitative PCR for *PDR2* in aboveground parts of 14-day-old seedlings and in different organs of a 2-month-old plant. Abbreviations: seedling (Seedl), flower (Flow), leaf margin (L mar) and leaf inner part (L inn), leaf devoid of trichomes (L – T) and trichomes (Trich). (b) Quantitative *PDR2* PCR in 24-day-old seedling root (light grey) and shoot (dark grew) treated with water, salicylic acid (SA), methyl jasmonate (MJA), abscisic acid (ABA), auxin (NAA), yeast extract (Yex), mannitol (Man) and sodium chloride (NaCl). (a, b) Data are depicted as means ± SE of three technical replicates of one representative biological sample.

basal to the trichomes (Fig. 4c). In stem tissue, expression was likewise restricted to trichomes (Fig. 4d). Belowground, promoter activity was pronounced in and around developing and emerging lateral root primordia (Fig. 4e), *PhPDR2* transcripts were also detected in flower tissue, particularly the stigma (Fig. 4f).

To determine elements regulating *PhPDR2* expression, its transcriptional response to various biotic and abiotic stress treatments was monitored. Pathogens commonly elicit a SA-dependent response, whereas herbivores elicit a JA-dependent response (Smith *et al.* 2009). Thus, the response of *PhPDR2* to SA and JA was investigated. In addition, the response to yeast extract, serving as a general fungal elicitor, was tested. To examine putative implications of *PhPDR2* in abiotic stress responses, we analyzed its transcript levels in response to

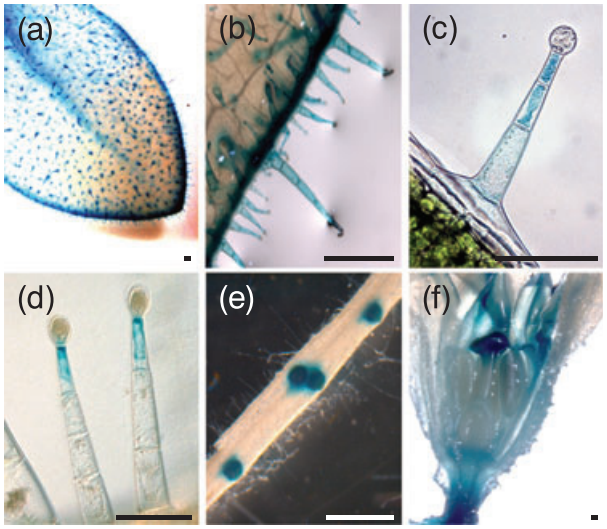

Figure 4. Tissue-specific expression of *PDR2*. GUS expression of a 2-month-old W115 *PDR2*::GUS in leaf (a), in leaf trichomes (b,c), in stem trichomes (d), in the main root (e) and in a flower (f). Scale bars are 1 mm. No background staining was observed in plants not expressing GUS using the same conditions as for GUS expressing plants.

ABA, a phytohormone involved in water stress, the auxin analogue 1-naphtaleneacetic acid (NAA), the osmotic stress inducer mannitol and sodium chloride, causing salt stress (Fig. 3b). *PhPDR2* transcripts accumulated markedly in seedling roots and shoots treated with MJA, suggesting an involvement in herbivore defense. However, in mature plants, this induction was not observed anymore (Supplemental Figure 4d–g). NtPDR5, previously reported to be involved in herbivore defense, was reported to be induced similarly upon JA treatment, but also upon mechanical wounding or application of oral secretion of *M. sexta* larvae, a Solanaceae specialist (Bienert *et al.* 2012). The transcriptional response of *PhPDR2* to the aforementioned treatments was investigated, and it was found that *PhPDR2* is not responsive to mechanical wounding or to the application of *M. sexta* oral secretion (Supplemental Figure 4e–g).

pdr2 lines are less toxic to caterpillars

For functional analysis of *PhPDR2*, *P. hybrida* W115 plants were transformed with a *PhPDR2*-RNAi construct. The three *PhPDR2*-RNAi lines $pdr2^1$, $pdr2^2$ and $pdr2^3$, displaying high to moderate *PhPDR2* transcript silencing, were chosen for further analysis (Fig. 5a). To test the hypothesis that PhPDR2 is involved in herbivore defense, caterpillars of the generalist herbivore *S. littoralis* were fed on *pdr2* leaves and on the respective wild-type leaves. Larval mortality and larval weight were monitored for larvae initially displaying the same average weight. Larval mortality rates were lower for larvae feeding on *pdr2* lines at all examined time points (Fig. 5b) and from day 9 until day 13 of feeding, significantly higher average weight was measured for larvae feeding on *pdr2* leaves as compared to such feeding on wild-type leaves (Fig. 5c). For example on day 13, chances of survival were nine times higher on *pdr2* than on wild-type leaves, and larval weight was 3.8-fold higher.

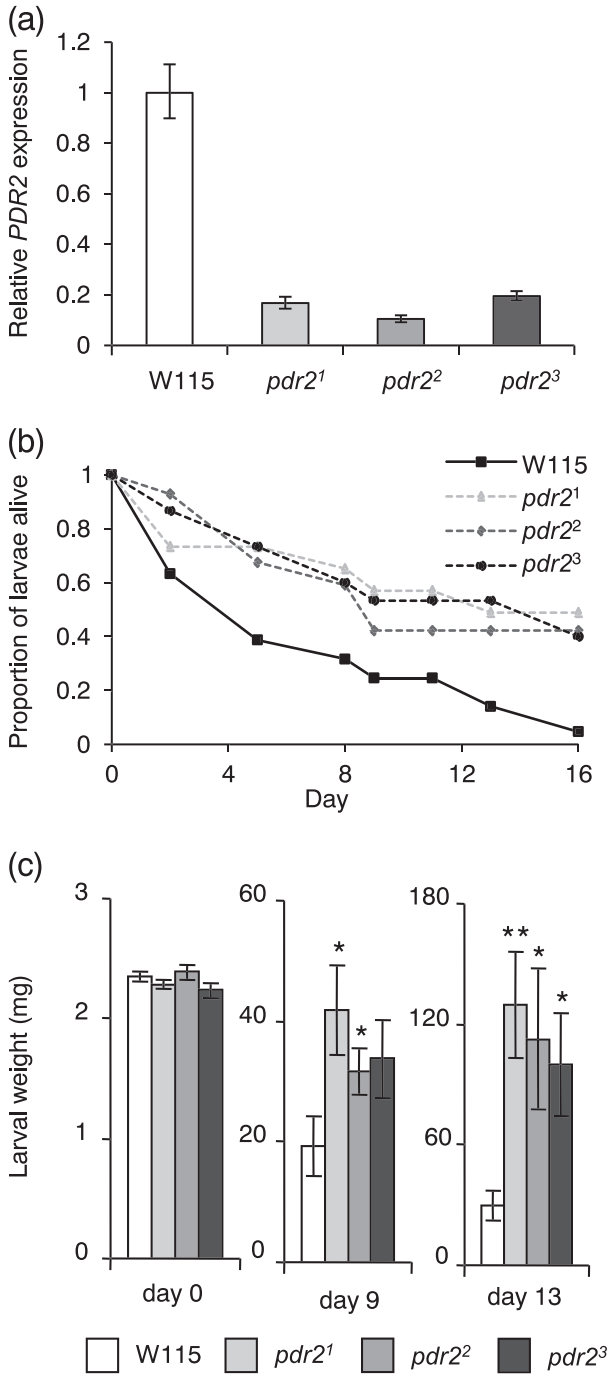

Figure 5. *Spodoptera littoralis* feeding on *pdr2* and wild type plants. (a) Quantitative PCR shows down-regulation of PDR2 in *pdr2* lines compared to wild type. (b, c) *Spodoptera littoralis* second instar larvae feeding experiments over 16 days on 3-month-old *pdr2* lines 1–3 (grey bars and symbols) or on wild type (white bars and symbols). Depicted are survival rate over time (b) and weight gain over time (b, means ± SE, 30 biological replicates, $\alpha = 0.05$). The experiments shown are representatives for three experiments performed.

Decreased metabolite contents in *pdr2* lines

PDR proteins related to *PhPDR2* have been shown to be involved in sclareol transport (Jasinski *et al.* 2001; Kang *et al.* 2011). *PhPDR2*, however, did not show a transcriptional response to sclareol and *pdr2* lines did not show an increased susceptibility to sclareol as compared to wild-type (Supplemental Figure 5), making implications of PhPDR2 in sclareol transport unlikely.

Instead of testing of additional single substrates, we decided to undertake an untargeted metabolomics profiling for PhPDR2 substrate identification. Briefly, *pdr2* and wild-type leaves were incubated in an organic solvent mixture, concentrated, and analyzed using ultra-high performance liquid chromatography coupled with high-resolution mass spectrometry (UHPLC-HR-MS). Unsupervised principal component analysis revealed 15 conspicuous candidate masses with MS signal intensities lower than 50% in two or more *pdr2* lines compared to the wild type. In order to improve the tracking of reduced metabolites, a two-group processing with the XCMS platform (see methods) was used and included feature detection, retention time correction, alignment, annotation and statistical analysis (Tautenhahn *et al.* 2012). Data obtained revealed 57 features with fold ≤ 0.66, *P*-values ≤ 0.01 and intensities ≥ 1000. Grouping the features, considering their accurate masses and generating chemical formulae allowed the attribution of 28 of them to 11 petuniasterone and petuniolide derivatives (Table 1, Supplemental Table 1). The structures of the most abundant plant steroids were further confirmed by MS/MS in comparison with data obtained from reference petuniasterone A (Fig. 6, Supplemental Figure 6). The compounds detected are present in several Petunia species, among them *P. hybrida* (Elliger *et al.* 1988a; Elliger *et al.* 1989a,1989b), and exhibit a strong insecticide activity. Furthermore, the XCMS processing revealed 29 features corresponding to 18 reduced metabolites that could not be identified so far (Supplemental Table 2).

To investigate whether the reduction of the steroidal compounds in *pdr2* lines was specific or if secondary metabolite levels in general were lower, we decided to further quantify a quercetin and a kaempferol galactopyranosides, two flavonoids that are well investigated in petunia (Zerback *et al.* 1989). Both were detected in similar amounts in *pdr2* and wild type, suggesting that the lower amounts of petuniasterones and petuniolides in *pdr2* lines were a specific effect (Table 1, Supplemental Table 1).

Finally, the relative concentrations of ca. 50 different plant steroids that have been characterized in several *Petunia* species, such as *P. hybrida, P. integrifolia, P. inflata, P. axillaris* and *P. parodii* were estimated. Because some of them share the same chemical formula, 37 extracted ion chromatograms (EICs) were calculated out of the UHPLC-HR-ESI-MS data. This data processing allowed for the detection of 62.2% of reported petuniasterone and petuniolide derivatives, whereof 65.2% were of lower intensities in *pdr2* leaves compared to wild-type leaves (Supplemental Table 2).

To test whether differential petuniolide and petuniasterone contents between wild-type and *pdr2* were reflected on the whole leaf level, we performed UHPLC-HR-M-based quantification on the inner leaf lamina and leaf margins. Leaf margins were assessed separately because they showed a strong *PhPDR2*-Promoter GUS signal. Congruent with findings for trichomes (Table 1), petuniolides A, C, E were highly abundant and were found at significantly lower amounts in *pdr2* lines as

Table 1. Petuniasterone and petuniolide content reduction in pools of *pdr2* lines

Substance	Feature ID	Fold[a]	*p*-Value	m/z_{med}	m/z_{theo}	Accuracy [μg g^{-1}]	Chemical formula	Rt_{med} (min)	Intensity	Adduct/fragment
Petuniolide E	#69	0.31	8.44E – 04	391.2632	391.2632	**0.0**	$C_{27}H_{35}O_2$	**5.83**	3044	$[M + H\text{-}AcOH\text{-}2H_2O]^+$
	#55	0.31	4.76E – 04	409.2742	409.2737	**−1.1**	$C_{27}H_{37}O_3$	**5.83**	2965	$[M + H\text{-}AcOH\text{-}H_2O]^+$
	#58	0.29	5.37E – 04	427.2843	427.2843	**0.1**	$C_{27}H_{39}O_4$	**5.83**	15961	$[M + H\text{-}AcOH]^+$
	#39	0.29	2.95E – 04	487.3044	487.3054	**2.1**	$C_{29}H_{43}O_6$	**5.83**	31407	$[M + H]^+$
	#28	0.22	1.59E – 04	504.3325	504.3320	**−1.1**	$C_{29}H_{46}O_6N$	**5.83**	1028	$[M + NH_4]^+$
	#64	0.21	6.60E – 04	509.2878	509.2874	**−0.8**	$C_{29}H_{42}O_6Na$	**5.83**	1180	$[M + Na]^+$
	#117	0.07	2.23E – 03	990.6296	990.6301	**0.5**	$C_{58}H_{88}O_{12}N$	**5.83**	3572	$[2\,M + NH_4]^+$
	Avg:	**0.19**	**7.43E – 04**	—	—	**—**	—	**—**	**59157**	= Σ intensities
Petuniolide A	#14	0.40	4.97E – 05	425.2686	425.2686	**0.1**	$C_{27}H_{37}O_4$	**5.29**	25835	$[M + H\text{-}2AcOH]^+$
	#1	0.32	3.25E – 07	485.2896	485.2898	**0.3**	$C_{29}H_{41}O_6$	**5.31**	5914	$[M + H\text{-}AcOH]^+$
	#4	0.32	3.17E – 06	562.3345	562.3374	**5.3**	$C_{31}H_{48}O_8N$	**5.30**	2977	$[M + NH_4]^+$
	#2	0.29	3.99E – 07	567.2923	567.2928	**0.9**	$C_{31}H_{44}O_8Na$	**5.30**	1374	$[M + Na]^+$
	Avg:	**0.33**	**1.34E – 05**	—	—	—	—	—	**36100**	= Σ intensities
Petuniolide F3	#355	0.38	8.15E – 03	503.3002	503.3003	**0.3**	$C_{29}H_{43}O_7$	**5.00**	9692	$[M + H]^+$
	#373	0.37	8.69E – 03	443.2786	443.2792	**1.4**	$C_{27}H_{39}O_5$	**5.00**	6802	$[M + H\text{-}AcOH]^+$
	Avg:	**0.37**	**8.42E – 03**	—	—	**—**	—	**—**	**16494**	: Σ intensities
Petuniasterone I/P3	#165	0.60	3.21E – 03	633.3083	633.3092	**1.4**	$C_{34}H_{49}O_9S$	**5.46**	4601	$[M + H]^+$
	#244	0.63	5.54E – 03	650.3341	650.3357	**2.6**	$C_{34}H_{52}O_9SN$	**5.46**	5587	$[M + NH_4]^+$
	#135	0.61	2.64E – 03	655.2899	655.2911	**1.8**	$C_{34}H_{48}O_9SNa$	**5.46**	4079	$[M + Na]^+$
	Avg:	**0.61**	**3.80E – 03**	—	—	**—**		**—**	**14267**	= Σ intensities
Petuniasterone G1/G2	#427	0.24	9.97E – 03	407.2940	407.2945	**1.1**	$C_{28}H_{39}O_2$	**4.22**	1631	$[M + H\text{-}3H_2O]^+$
	#365	0.22	8.44E – 03	425.3048	425.3050	**0.6**	$C_{28}H_{41}O_3$	**4.22**	3535	$[M + H\text{-}2H_2O]^+$
	#318	0.19	7.22E – 03	443.3146	443.3156	**2.3**	$C_{28}H_{43}O_4$	**4.22**	6640	$[M + H\text{-}H_2O]^+$
	#335	0.18	8.24E – 03	461.3301	461.3262	**−8.6**	$C_{28}H_{45}O_5$	**4.22**	2346	$[M + H]^+$
	Avg:	**0.20**	**8.47E – 03**	—	—	**—**	—	**—**	**14152**	= Σ intensities
Petuniolide F2	#87	0.45	1.38E – 03	503.3004	503.3003	**−0.1**	$C_{29}H_{43}O_7$	**4.70**	9201	$[M + H]^+$
	#122	0.45	2.33E – 03	443.2785	443.2792	**1.6**	$C_{27}H_{39}O_5$	**4.70**	2670	$[M + H\text{-}AcOH]^+$
	Avg:	**0.45**	**1.86E – 03**	—	—	**—**	—	**—**	**11871**	= Σ intensities
Petuniolide C	#416	**0.17**	**9.71E – 03**	501.2851	501.2847	**−0.9**	$C_{29}H_{41}O_7$	**4.86**	**9891**	$[M + H]^+$
Petuniolide F1	#32	0.28	1.75E – 04	503.3001	503.3003	**0.4**	$C_{29}H_{43}O_7$	**5.99**	6384	$[M + H]^+$
	#65	0.37	7.44E – 04	443.2774	443.2792	**4.1**	$C_{27}H_{39}O_5$	**5.99**	3476	$[M + H\text{-}AcOH]^+$
	Avg:	**0.32**	**4.60E – 04**	—	—	**—**	—	**—**	**9860**	= Σ intensities
Petuniasterone L/R	#33	0.40	1.99E – 04	615.2970	615.2986	**2.6**	$C_{34}H_{47}O_8S$	**5.63**	4144	$[M + H]^+$
	#107	0.41	1.83E – 03	615.2973	615.2986	**2.2**	$C_{34}H_{47}O_8S$	**5.25**	1671	$[M + H]^+$
	Avg:	**0.41**	**1.02E – 03**	—	—	**—**	—	**—**	**5815**	= Σ intensities
Perulactone C/D	#381	**0.19**	**8.94E – 03**	535.3254	535.3265	**2.2**	$C_{30}H_{47}O_8$	**4.59**	**1577**	$[M + H]^+$
Petuniasterone H	#44	**0.20**	**3.35E – 04**	521.3458	521.3473	**2.8**	$C_{30}H_{49}O_7$	**4.78**	1402	$[M + H]^+$
Q-3-GluGal	#3794[a]	0.85	5.05E – 01	625.1415	625.1410	**−0.8**	$C_{27}H_{29}O_{17}$	**2.20**	**16319**	$[M - H]^-$
K-3-GluGal	#4420	0.91	6.03E – 01	609.1467	609.1461	**−1.0**	$C_{27}H_{29}O_{16}$	**2.35**	**9002**	$[M - H]^-$

Greenhouse-grown leaves were washed in buffer and metabolites were analyzed using the XCMS platform.

List of substances with the feature ID assigned by XCMS analysis, as well as the fold reduction and the *p*-value (data displayed is median of three *pdr2* lines), the measured mass (*m/z* med), the mass accuracy, retention time (RT med) and intensity. Chemical formula and accuracy were calculated with the SmartFormula software. For steroids with more than one feature, the average of the fold reduction, *p*-value, and the sum of the intensities are given in addition in bold. In addition to steroids, amounts of two flavonoids, Q-3-GluGal and K-3-GluGal (Quercetin 3-*O*-(2″-*O*-*β*-D-glucopyranosyl)-*β*-D-galactopyranoside and Kaempferol 3-*O*-(2″-*O*-*β*-D-glucopyranosyl)-*β*-D-galactopyranoside, respectively (Zerback *et al.* 1989)) were analyzed. Analysis of unknown metabolites can be found in Supplemental Table 2.

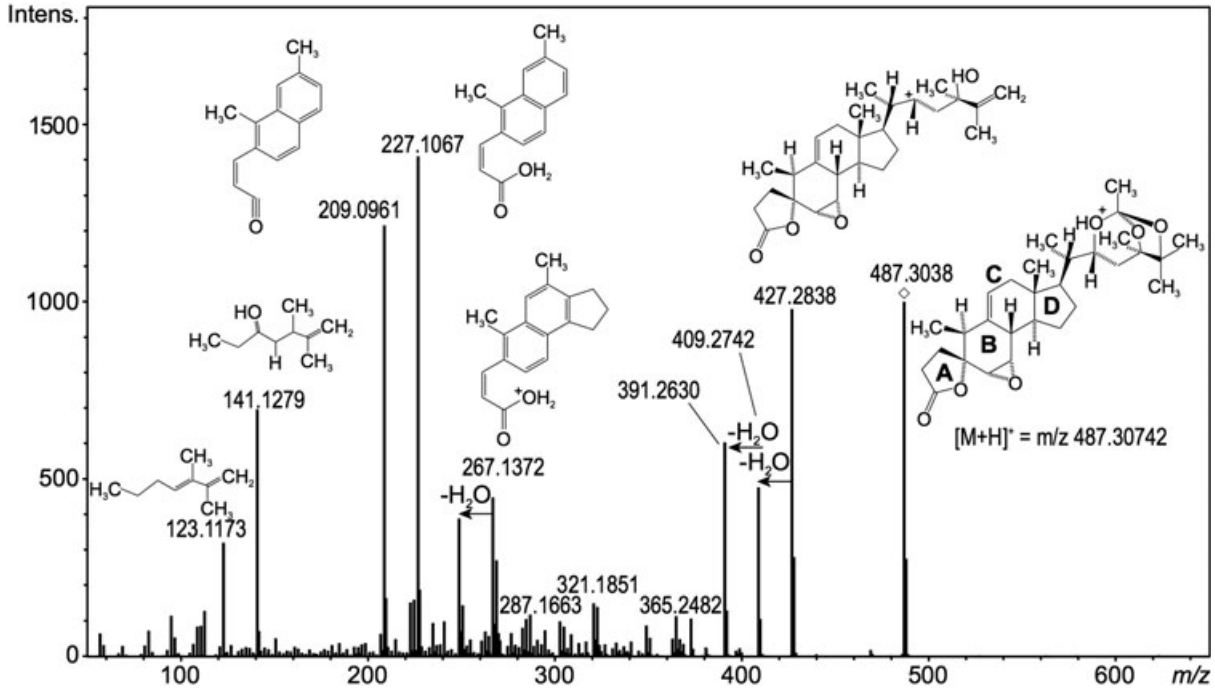

Figure 6. Petuniasterone MS/MS studies. MS/MS peaks and predicted corresponding fragment structures for Petuniolide E, a toxic steroidal compound found at lower concentrations in *pdr2* lines.

compared to the wild-type ($p < 0.0005$). The less abundant petuniolides F1–4 were also significantly reduced in *pdr2* ($p < 0.0005$) compared to wild type samples, a trend also observed for petuniasterones A acetate, G1/G2 and I/P3 (Fig. 7, Supplemental Figure 7). The two orders of magnitude difference in signal intensities between petuniolide E and petuniasterone H in whole leaf extracts were consistent with the findings for trichome extracts (Supplemental Table 1). Interestingly, levels of the highest abundant petuniasterone, petuniasterone L/R, did not differ between *pdr2* and wild type samples, indicating an accumulation independent of PhPDR2 (Fig. 7).

Petuniolide A was significantly more abundant in the marginal areas for both wild type ($p = 0.01$) and *pdr2* ($p = 0.006$), when compared to inner leaf lamina. For the other petuniolides, the differences between inner leaf lamina and leaf margin were not significant in the wild type, while they were significant in *pdr2* ($p < 0.01$). The different Petuniolid A distribution observed in leaf lamina and margins might be dependent on differences in trichome abundance or *PhPDR2* expression patterns, as *PhPDR2* is expressed in both cell types. Therefore, we quantified trichome density in leaf lamina and margins, both on adaxial and abaxial sides. No significant differences in trichome density were scored (521 +/− 95 adaxial lamina; 764 +/− 162 abaxial lamina; 850 +/− 142 adaxial margin; 925 +/− 147 abaxial margin; $n = 12$. *P* value adaxial lamina to margin = 0.08; *p* value abaxial lamina to margin = 0.47). Therefore, we suggest that *PhPDR2* expression at the leaf borders is responsible for the higher accumulation of steroidal compounds at the margins, compatible with PhPDR2 function against herbivore attacks.

DISCUSSION

PhPDR2 is a PDR/ABCG protein expressed in glandular trichomes of leaves and stem

Toxic or deterrent secondary metabolites have been recognized as important means for herbivory defense (Schilmiller *et al.* 2008), and they are commonly found in high concentrations at exposed sites, such as the heads of glandular trichomes (Shroff *et al.* 2008; Weinhold & Baldwin 2011) and leaf margins (Schweizer *et al.* 2013). Postulating functional implications of primary active secondary metabolite transport to build up and maintain concentration gradients across membranes at glandular trichomes, we decided to screen for PDR transporters of petunia (Supplemental Figure 1) that are preferentially expressed in trichomes.

Four new petunia PDR sequences were identified and brought into phylogenetic context with characterized members of the PDR subclass (Fig. 1), revealing the absence of close homologues for PhPDR2. PhPDR2 is a typical PDR/full-size ABCG protein featuring a reverse domain orientation (Supplemental Figure 3b) and localizing to the plasma membrane (Fig. 2). Distinct expression of *PhPDR2* in leaf borders and trichomes was demonstrated by RT-PCR (Fig. 4a) and GUS reporter studies (Fig. 4). Congruence of both approaches suggests that the promoter region used correctly targets *PhPDR2* expression. *PhPDR2* is expressed in all stalk cells of the trichome (Fig. 4c–d). Collectively, this data points towards a contribution of PhPDR2 in the export of substances from trichomes into the apoplastic space, possibly enhanced in proximity to the glandular head.

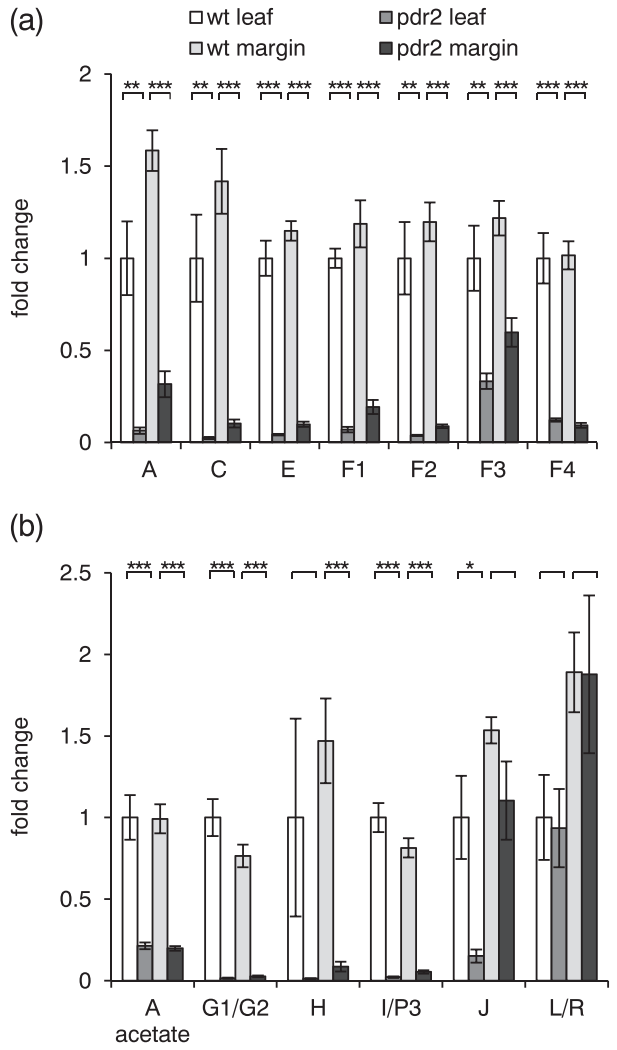

Figure 7. Relative petuniolide (a) and petuniasterone (b) levels in leaves and leaf margins of wild type and *pdr2* plants. Petuniolide (a) and petuniasterone (b) amounts as detected by UHPLC HR-MS in wild type and *pdr2* leaf lamina and margins (wt lamina, white; pdr2 lamina, grey; wt margin, light grey; pdr2 margin, dark grey). Values are expressed as means ± SE, $n = 6$ (* $p < 0.05$; ** $p < 0.005$; *** $p < 0.0005$). Values are normalized to wild type lamina levels. Absolute values are depicted in Supplemental Figure 7.

A role for *PhPDR2* in herbivory

To date, NtPDR5 is the only plant transporter reportedly involved in herbivore defense. Similar to *pdr2*, *Ntpdr5* plants are more susceptible to herbivore feeding (Bienert *et al.* 2012). However, unlike *PhPDR2*, *NtPDR5* is induced in leaf tissue upon mechanical wounding, application of *M. sexta* oral secretion or feeding (Supplemental Figure 4) (Bienert *et al.* 2012). The differences in expression of *PhPDR2* and *NtPDR5*, as well as their distant phylogenetic relationship (Fig. 1, Supplemental Figure 2), suggest deviating roles in defense responses. The expression pattern of *PhPDR2* suggests an involvement as a constitutive and unspecific component as a first line of defense in trichomes and the leaf borders. Although up-regulated by JA at the seedling stage, PhPDR2 is unresponsive to chemical or mechanical feeding stimuli. *Nt*PDR5, on the other hand, appears to be part of an inducible defense strategy that works locally at sites of attack. Our results underline the importance of active transport of secondary metabolites across trichome cells in plant defense against herbivores.

Insecticidal petuniasterone and petuniolide contents are lower in *pdr2* lines

A first attempt to identify potential substrates of PhPDR2 involved a targeted approach. Close relatives of PhPDR2 have been implicated in terpenoid or sclareol transport (Jasinski *et al.* 2001; van den Brule *et al.* 2002; Campbell *et al.* 2003; Crouzet *et al.* 2013). However, we could not observe a difference between wild-type and *pdr2* lines in various sclareol assays (Supplemental Figure 5). Metabolite contents of wild-type and *pdr2* lines were analyzed with UHPLC-HR-MS and revealed the presence of several secondary metabolites reduced in *pdr2* lines, among them many steroidal compounds (Table 1, Supplemental Tables 1 and 2). The levels of two flavonoids remained unchanged, corroborating the specificity of *pdr2* involvement in steroidal compound transport (Table 1, Supplemental Table 1). The accurate masses and the resulting chemical formulae of several candidates are corresponding to petuniasterones and petuniolides, both steroidal compounds (Table 1, Supplemental Tables 1 and 2). MS/MS confirmed their structures, in particular comparison of the fragmentation pattern of extracted petuniasterone A acetate with petuniasterone A reference material (Supplemental Figure 6).

Petuniasterones were firstly identified 1988 in petunia leaves (Elliger *et al.* 1988b; Elliger *et al.* 1989a) within a screen for substances exhibiting toxicity to insect larvae. These compounds contained a ketone moiety at the A-ring and were therefore termed petuniasterones (Supplemental Table 1). Later, the structure of a second class of steroidal compounds with a spiro-lactone A-ring was described and called petuniolides (Supplemental Table 1).

Petuniasterones with a linear side chain (e.g. petuniasterone H, Supplemental Figure 6) are not toxic to insects, whereas orthoester derivatives (e.g. petuniasterone A) are toxic against a wide variety of caterpillars, among them the *Solanaceae* specialist *M. sexta*, or the *Spodoptera sp.* generalists (Elliger & Waiss 1991). In our experiments, we find both, petuniasterones with linear and orthoester side chains to be present in lower amounts in *pdr2* lines. Petuniolides typically have an orthoester side chain, and a rearranged sterol backbone containing lactone ring. In general, petuniolides are about 10-fold more toxic than petuniasterones (Elliger & Waiss 1991). A possible mode of action was proposed for petuniolides C and D, which were shown to be weak ligands of rat brain GABA receptors (Isman *et al.* 1998). Cockroaches with a mutated GABA receptor were less susceptible to various insecticides and displayed elevated resistance against petuniolides (Isman *et al.* 1998).

We found several petuniolides and petuniasterones with high intensity to be significantly reduced in *pdr2* lines

(Table 1), irrespective of the sampling method (for trichomes, see Table 1, for leaf lamina and leaf margins, see Fig. 7 and Supplemental Figure 7). Trichomes, major sites of *PhPDR2* expression (Fig. 4b–d), are recognized to play an important role in herbivore defense (Wang *et al.* 2001; Yazaki 2006; Schilmiller *et al.* 2008; Slocombe *et al.* 2008; Loreto *et al.* 2014). Leaf margins also express *PhPDR2* (Fig. 4a), and they were also reported to have insecticidal properties. In Arabidopsis, specific accumulation of insecticidal glucosinolate in leaf margins has been reported (Schweizer *et al.* 2013). The same report identified leaf margins as preferential feeding sites of *S. littoralis* once the glucosinloate biosynthesis was impaired. Most of the petuniolides and petuniasterones were indeed found to be more abundant in the leaf margins as compared to the inner leaf lamina though in the wild type the differences were significant only for petuniolide A (Fig. 7, Supplemental Figure 7). The high abundance of petuniolides A, C and E in leaf margins might be implicated in warding off generalists like *S. littoralis* that tend to prefer to feed on the margins if they are not particularly protected. Thus, the function of petuniolides in petunia would be similar to the observed function of glucosinolate in leaf margins of Arabidopsis (Schweizer *et al.* 2013). Indeed, we found that *S. littoralis* feeding on *pdr2* leaves to gain weight faster and to survive better than larvae feeding on wild type leaves (Fig. 6). As both, petuniasterone and petuniolide levels are reduced in *pdr2* lines; larvae feeding on *pdr2* leaves ingests less toxic compounds per unit leaf material.

Petuniolide C was suggested to be the most relevant substance in *P. parodii* because of its high toxicity and abundance (Elliger & Waiss 1991) (Dereeper *et al.* 2008). We also identified petuniolide C in our samples, although in lower amounts than petuniolide A or E (Supplemental Figure 7). Given their high abundance and toxicity and their high decrease in *pdr2*, however, these three compounds are likely the main contributors to the observed herbivory phenotype. The contrast to published data could be because of different metabolite abundance in *P. hybrida*, or because of the slightly different growth condition or extraction methods. Although most petuniasterones and petuniolides were reduced in *pdr2* lines, not all levels were lover in *pdr2* lines (Supplemental Table 2, Fig. 7), which could indicate a specificity of PhPDR2 for selected molecules or precursors. In addition, not all reported petuniasterones and petuniolides were identified in our experiments, and it should be kept in mind that besides masses corresponding to known petuniasterones and petuniolides, around 18 further down-regulated components were present in lower amounts in *pdr2* lines (Supplemental Table 2). The corresponding chemical formulae have not been described for petunia so far, and the structures could not be elucidated with MS/MS experiments. Therefore, we cannot exclude that some of them may also be involved in PhPDR2-mediated herbivore resistance of petunia.

To address exact function of *PhPDR2* expression around emerging lateral roots and in floral reproductive tissues (Fig. 4e–f), additional studies are needed. It is possible that petuniolides are exuded in the rhizosphere to protect emerging later roots from belowground herbivory; however, in the case of the stigma, exudation of insecticidal compounds would be highly detrimental for an insect-pollinated plant such as petunia.

Petuniasterones and petuniolides have a sterol backbone. Sterol transporters were firstly identified in humans and yeast. Heterodimers of human ABCG5 and ABCG8 are responsible for cholesterol and phytosterol export from the liver to the bile (Klett & Patel 2003; Moitra *et al.* 2011; Tarling *et al.* 2013) and mutations in either cause sitosterolemia, a disease characterized by the failure of cholesterol and phytosterol excretion (Wittenburg & Carey 2002). About half of the 20 characterized ABC members of humans are involved in transport of lipids or lipid-derived compounds, and the proteins are either localized in the plasma membrane or in endosomal compartments (Tarling *et al.* 2013). Similarly, in yeast, ABCG proteins have been reported to be involved in cholesterol, phytosterol and ergosterol transport, the latter being a structural sterol (Li 2004; Jungwirth & Kuchler 2006; Cabrito *et al.* 2011). In *A. thaliana*, ABCG9 and ABCG31 were very recently reported to be involved in steryl-glycoside deposition in pollen (Choi *et al.* 2014). The finding that a large number of ABCG-type ABC transporters is likely to act as sterol transporters supports the hypothesis of PhPDR2 being a sterol transporter involved in the export of petuniasterones and petuniolides. However, because of the fact that these compounds are not commercially available, we were unable to provide direct proof via transport assays. A further obstacle in directly demonstrating transport activity is the hydrophobicity of these compounds, which is the reason, why direct evidence was also not provided for other Arabidopsis transporting lipidic compounds.

We conclude that *P. hybrida* PhPDR2 is a trichome and leaf-margin-localized plasma-membrane intrinsic protein with a major role in herbivore defense against generalist feeders. Considering demonstrated affinities of ABCG transporters for steroidal compounds across kingdoms and the finding that down-regulation of *PhPDR2* is associated with reduced amounts of petuniasterones and petuniolides, we postulate that PhPDR2 is involved in the export of steroidal, insecticidal compounds.

ACKNOWLEDGMENTS

We thank Christian Gübeli for technical support, and Prof. Ian Baldwin from the Max Planck Institute for Chemical Ecology in Jena, Germany for the supply of *Manduca sexta* oral secretion. This work was supported by the Swiss National Foundation within the NCCR Plant Survival.

GENBANK ACCESSION NUMBER

BankIt1891159 PHPDR2 KU665392

AUTHOR CONTRIBUTIONS

E.M., J.S., L.Bi. and T.K. designed the research, J.S., M.S., M. L., L.Bo., G.W., L.Bi. and T.K. performed the research, J.G. and L.Bi contributed new analysis tools and J.S., L.Bi, E.M. and T.K. wrote the publication.

REFERENCES

Badri D.V., Loyola-Vargas V.M., Broeckling C.D., De-la-Pena C., Jasinski M., Santelia D., … Vivanco J.M. (2008) Altered profile of secondary metabolites in the root exudates of Arabidopsis ATP-binding cassette transporter mutants. *Plant Physiology* **146**, 762–771.

Banasiak J., Biala W., Staszkow A., Swarcewicz B., Kepczynska E., Figlerowicz M. & Jasinski M. (2013) A *Medicago truncatula* ABC transporter belonging to subfamily G modulates the level of isoflavonoids. *Journal of Experimental Botany* **64**, 1005–1015.

Becker D., Kemper E., Schell J. & Masterson R. (1992) New plant binary vectors with selectable markers located proximal to the left T-DNA border. *Plant Molecular Biology* **20**, 1195–1197.

Besser K., Harper A., Welsby N., Schauvinhold I., Slocombe S., Li Y., … Broun P. (2009) Divergent regulation of terpenoid metabolism in the trichomes of wild and cultivated tomato species. *Plant Physiology* **149**, 499–514.

Bessire M., Borel S., Fabre G., Carraca L., Efremova N., Yephremov A., … Nawrath C. (2011) A member of the PLEIOTROPIC DRUG RESISTANCE family of ATP binding cassette transporters is required for the formation of a functional cuticle in arabidopsis. *The Plant Cell* **23**, 1958–1970.

Bienert M.D., Siegmund S.E., Drozak A., Trombik T., Bultreys A., Baldwin I.T. & Boutry M. (2012) A pleiotropic drug resistance transporter in *Nicotiana tabacum* is involved in defense against the herbivore *Manduca sexta*. *The Plant Journal* **72**, 745–757.

Bleeker P.M., Mirabella R., Diergaarde P.J., VanDoorn M., Tissier A., Kant M.R., … Schuurink R.C. (2012) Improved herbivore resistance in cultivated tomato with the sesquiterpene biosynthetic pathway from a wild relative. *Proceedings of the National Academy of Sciences of the United States of America* **109**, 20124–20129.

Bodenhausen N. & Reymond P. (2007) Signaling pathways controlling induced resistance to insect herbivores in Arabidopsis. *Molecular Plant Microbe Interactions* **20**, 1406–1420.

Cabrito T.R., Teixeira M.C., Singh A., Prasad R. & Sà C.I. (2011) The yeast ABC transporter Pdr18 (ORF YNR070w) controls plasma membrane sterol composition, playing a role in multidrug resistance. *Biochemical Journal* **440**, 195–202.

Campbell E.J., Schenk P.M., Kazan K., Penninckx I.A., Anderson J.P., Maclean D.J., … Manners J.M. (2003) Pathogen-responsive expression of a putative ATP-binding cassette transporter gene conferring resistance to the diterpenoid sclareol is regulated by multiple defense signaling pathways in Arabidopsis. *Plant Physiology* **133**, 1272–1284.

Chen G., Komatsuda T., Ma J.F., Nawrath C., Pourkheirandish M., Tagiri A., … Nevo E. (2011) An ATP-binding cassette subfamily G full transporter is essential for the retention of leaf water in both wild barley and rice. *Proceedings of the National Academy of Sciences of the United States of America* **108**, 12354–12359.

Choi H., Ohyama K., Kim Y.Y., Jin J.Y., Lee S.B., Yamaoka Y., … Lee Y. (2014) The role of arabidopsis ABCG9 and ABCG31 ATP binding cassette transporters in pollen fitness and the deposition of steryl glycosides on the pollen coat. *The Plant Cell* **26**, 310–324.

Crouzet J., Roland J., Peeters E., Trombik T., Ducos E., Nader J. & Boutry M. (2013) NtPDR1, a plasma membrane ABC transporter from *Nicotiana tabacum*, is involved in diterpene transport. *Plant Molecular Biology* **82**, 181–192.

Crouzet J., Trombik T., Fraysse A.S. & Boutry M. (2006) Organization and function of the plant pleiotropic drug resistance ABC transporter family. *FEBS Letters* **580**, 1123–1130.

Cutler H.G., Reid W.W. & Delétang J. (1977) Plant-growth inhibiting properties of diterpenes from tobacco. *Plant and Cell Physiology* **18**, 711–714.

Dereeper A., Guignon V., Blanc G., Audic S., Buffet S., Chevenet F., … Gascuel O. (2008) Phylogeny.fr, robust phylogenetic analysis for the non-specialist. *Nucleic Acids Research* **36**, W465–W469.

Ducos E., Fraysse S. & Boutry M. (2005) NtPDR3, an iron-deficiency inducible ABC transporter in *Nicotiana tabacum*. *FEBS Letters* **579**, 6791–6795.

Eichhorn H., Klinghammer M., Becht P. & Tenhaken R. (2006) Isolation of a novel ABC-transporter gene from soybean induced by salicylic acid. *Journal of Experimental Botany* **57**, 2193–2201.

Elliger C.A., Benson M., Haddon W.F., Lundin R.E., Waiss A.C. & Wong R.Y. (1989a) Petuniasterones. Part 2. Novel ergostane-type steroids from *Petunia hybrida* vilm. (solanaceae). *Journal of the Chemical Society, Perkin Transactions* **1**, 143–149.

Elliger C.A., Benson M., Lundin R.E. & Waiss A.C.J. (1988a) Minor Petuniasterones from *Petunia hybrida*. *Phytochemistry* **27**, 3597–3603.

Elliger C.A., Benson M.E., Haddon W.F., Lundin R.E., Waiss A.C. & Wong R.Y. (1988b) Petuniasterones, novel ergostane-type steroids of *Petunia hybridia* Vilm. (Solanaceae) having insect-inhibitory activity. X-ray molecular structure of the 22,24,25-[(methoxycarbonyl)orthoacetate] of 7a,22,24,25-tetrahydroxy ergosta-1,4-dien-3-one and of 1a-acetoxy-24,25-epoxy-7a-hydroxy-22-(methylthiocarbonyl)acetoxyergost-4-en-3-one. *Journal of the Chemical Society, Perkin Transactions* **1**, 711–717.

Elliger C.A. & Waiss A.C. Jr. (1991) *Insect Resistance Factors in Petunia*, ACS Symposium Series, pp. 210–223. American Chemical Society, Washington, DC.

Elliger C.A., Waiss A.C., Benson M. & Wong R.Y. (1990a) Ergostanoids from *Petunia parodii*. *Phytochemistry* **29**, 1–11.

Elliger C.A., Waiss A.C., Benson M. & Wong R.Y. (1993) Ergostanoids from *Petunia inflata*. *Phytochemistry* **33**, 471–477.

Elliger C.A., Waiss A.C.J. & Benson M. (1992) Petuniasterone R, a new ergostanoid from *Petunia parodii*. *Journal of Natural Products* **55**, 129–133.

Elliger C.A., Waiss A.C.J., Wong R.Y. & Benson M. (1989b) Petuniasterones from *Petunia parodii* and *P. integrifolia*; unusual ergostane-type steroids. *Phytochemistry* **28**, 3443–3452.

Elliger C.A., Wong R.Y., Waiss A.C. & Benson M. (1990b) Petuniolides. Unusual ergostanoid lactones from Petunia species that inhibit insect development. *Journal of the Chemical Society, Perkin Transactions* **1**, 525.

Galbiati M., Simoni L., Pavesi G., Cominelli E., Francia P., Vavasseur A., … Tonelli C. (2008) Gene trap lines identify Arabidopsis genes expressed in stomatal guard cells. *The Plant Journal* **53**, 750–762.

Gerats T. & Vandenbussche M. (2005) A model system for comparative research, Petunia. *Trends in Plant Science* **10**, 251–256.

Gershenzon J. & Dudareva N. (2007) The function of terpene natural products in the natural world. *Nature Chemical Biology* **3**, 408–414.

Guerineau F., Benjdia M. & Zhou D.X. (2003) A jasmonate-responsive element within the *A. thaliana* vsp1 promoter. *Journal of Experimental Botany* **54**, 1153–1162.

Hare J.D. (2005) Biological activity of acyl glucose esters from *Datura wrightii* glandular trichomes against three native insect herbivores. *Journal of Chemical Ecology* **31**, 1475–1491.

Hellens R.P., Edwards E.A., Leyland N.R., Bean S. & Mullineaux P.M. (2000) pGreen, a versatile and flexible binary Ti vector for Agrobacterium-mediated plant transformation. *Plant Molecular Biology* **42**, 819–832.

Howe G.A. & Jander G. (2008) Plant immunity to insect herbivores. *Annual Review of Plant Biology* **59**, 41–66.

Hwang J.U., Song W.-Y., Hong D., Ko D., Yamaoka Y., Jang S., … Lee Y. (2016) Plant ABC transporters enable many unique aspects of a terrestrial plant's lifestyle. *Molecular Plant* **9**, 338–355.

Isman M.B., Jeffs L.B., Elliger C.A., Miyake T. & Matsumura F. (1998) Petuniolides, natural insecticides from *Petunia parodii*, are antagonists of GABAa receptors. *Pesticide Biochemistry and Physiology* **58**, 103–107.

Ito H. & Gray W.M. (2006) A gain-of-function mutation in the Arabidopsis pleiotropic drug resistance transporter PDR9 confers resistance to auxinic herbicides. *Plant Physiology* **142**, 63–74.

Jasinski M., Stukkens Y., Degand H., Purnelle B., Marchand-Brynaert J. & Boutry M. (2001) A plant plasma membrane ATP binding cassette-type transporter is involved in antifungal terpenoid secretion. *The Plant Cell* **13**, 1095–1107.

Jungwirth H. & Kuchler K. (2006) Yeast ABC transporters—a tale of sex, stress, drugs and aging. *FEBS Letters* **580**, 1131–1138.

Kang J., Park J., Choi H., Burla B., Kretzschmar T., Lee Y. & Martinoia E. (2011) Plant ABC transporters. *Arabidopsis Book* **9**, e0153.

Kang J.H., Liu G., Shi F., Jones A.D., Beaudry R.M. & Howe G.A. (2010a) The tomato odorless-2 mutant is defective in trichome-based production of diverse specialized metabolites and broad-spectrum resistance to insect herbivores. *Plant Physiology* **154**, 262–272.

Kang J.H., Shi F., Jones A.D., Marks M.D. & Howe G.A. (2010b) Distortion of trichome morphology by the hairless mutation of tomato affects leaf surface chemistry. *Journal of Experimental Botany* **61**, 1053–1064.

Kim D.-Y., Bovet L., Maeshima M., Martinoia E. & Lee Y. (2007) The ABC transporter AtPDR8 is a cadmium extrusion pump conferring heavy metal resistance. *The Plant Journal* **50**, 207–218.

Klett E.L. & Patel S. (2003) Genetic defenses against noncholesterol sterols. *Current Opinion in Lipidology* **14**, 341–345.

Kobae Y., Sekino T., Yoshioka H., Nakagawa T., Martinoia E. & Maeshima M. (2006) Loss of AtPDR8, a plasma membrane ABC transporter of *Arabidopsis thaliana*, causes hypersensitive cell death upon pathogen infection. *Plant, Cell & Environment* **47**, 309–318.

Kretzschmar T., Burla B., Lee Y. & Martinoia E. (2011) Functions of ABC transporters in plants. *Essays in Biochemistry* **50**, 145–160.

Kretzschmar T., Kohlen W., Sasse J., Borghi L., Schlegel M., Bachelier J.B., … Martinoia M. (2012) A petunia ABC protein controls strigolactone-dependent symbiotic signalling and branching. *Nature* **483**, 341–344.

Kreuz K., Tommasini R. & Martinoia E. (1996) Old enzymes for a new job (herbicide detoxification in plants). *Plant Physiology* **111**, 349–353.
Lee J., Bae H., Jeong J., Lee J.Y. & Yang Y.Y. (2003) Functional expression of a bacterial heavy metal transporter in Arabidopsis enhances resistance to and decreases uptake of heavy metals. *Plant Physiology* **133**, 589–596.
Lee M., Lee K., Lee J., Noh E.W. & Lee Y. (2005) AtPDR12 contributes to lead resistance in Arabidopsis. *Plant Physiology* **138**, 827–836.
Li Y. (2004) ATP-binding cassette (ABC) transporters mediate nonvesicular, raft-modulated sterol movement from the plasma membrane to the endoplasmic reticulum. *Journal of Biological Chemistry* **279**, 45226–45234.
Loreto F., Dicke M., Schnitzler J.-P. & Turlings T.C.J. (2014) Plant volatiles and the environment. *Plant, Cell & Environment* **37**, 1905–1908.
Lutke W.K. (2006) Petunia (*Petunia hybrida*). *Methods in Molecular Biology* **344**, 339–349.
Martinoia E., Klein M., Geisler M., Bovet L., Forestier C., Kolukisaoglu Ü., … Schulz B. (2002) Multifunctionality of plant ABC transporters—more than just detoxifiers. *Planta* **214**, 345–355.
Moitra K., Silverton L., Limpert K., Im K. & Dean M. (2011) Moving out, from sterol transport to drug resistance—the ABCG subfamily of efflux pumps. *Drug Metabolism and Drug Interactions* **26**, 105–111.
Oerke E.C. (2005) Crop losses to pests. *Journal of Agricultural Science* **144**, 31.
Sasabe M., Toyoda K., Shiraishi T., Inagaki Y. & Ichinose Y. (2002) cDNA cloning and characterization of tobacco ABC transporter, NtPDR1 is a novel elicitor-responsive gene. *FEBS Letters* **518**, 164–168.
Schilmiller A.L., Last R.L. & Pichersky E. (2008) Harnessing plant trichome biochemistry for the production of useful compounds. *The Plant Journal* **54**, 702–711.
Schweizer F., Fernández-Calvo P. & Zander M. (2013) Arabidopsis basic helix–loop–helix transcription factors MYC2, MYC3, and MYC4 regulate glucosinolate biosynthesis, insect performance, and feeding behavior. *The Plant Cell* **25**, 3117–3132.
Shroff R., Vergara F., Muck A., Svatos A. & Gershenzon J. (2008) Nonuniform distribution of glucosinolates in *Arabidopsis thaliana* leaves has important consequences for plant defense. *Proceedings of the National Academy of Sciences of the United States of America* **105**, 6196–6201.
Slocombe S.P., Schauvinhold I., McQuinn R.P., Besser K., Welsbz N.A., Harper A., … Broun P. (2008) Transcriptomic and reverse genetic analyses of branched-chain fatty acid and acyl sugar production in *Solanum pennellii* and Nicotiana *benthamiana*. *Plant Physiology* **148**, 1830–1846.
Smith J.L., De Moraes C.M. & Mescher M.C. (2009) Jasmonate- and salicylate-mediated plant defense responses to insect herbivores, pathogens and parasitic plants. *Pest Managment Science* **65**, 497–503.
Stukkens Y., Bultreys A., Grec S., Trombik T., Vanham D. & Boutry M. (2005) NpPDR1, a pleiotropic drug resistance-type ATP-binding cassette transporter from *Nicotiana plumbaginifolia*, plays a major role in plant pathogen defense. *Plant Physiology* **139**, 341–352.
Tarling E.J., de Aguiar Vallim T.Q. & Edwards P.A. (2013) Role of ABC transporters in lipid transport and human disease. *Trends in Endocrinology & Metabolism* **24**, 342–350.
Tautenhahn R., Patti G.J., Rinehart D. & Siuzdak G. (2012) XCMS online, a Web-based platform to process untargeted metabolomic data. *Analytical Chemistry* **84**, 5035–5039.
Theodoulou F.L. (2000) Plant ABC transporters. *Biochimica et Biophysica Acta* **1465**, 79–7103.
Tissier A., Sallaud C. & Rontein D. (2013) Tobacco trichomes as a platform for terpenoid biosynthesis engineering. In *Isoprenoid Synthesis in Plants and Microorganisms* (eds Bach T.J. & Rohmer M.), pp. 271–283. Springer, New York.
Trombik T., Jasinski M., Crouzet J. & Boutry M. (2008) Identification of a cluster IV pleiotropic drug resistance transporter gene expressed in the style of *Nicotiana plumbaginifolia*. *Plant Molecular Biology* **66**, 165–175.
van Dam N.M. & Hare J.D. (1998) Biological activity of *Datura wrightii* glandular trichome exudate against *Manduca sexta* larvae. *Journal of Chemical Ecology* **24**, 1529–1549.
van den Brule S., Muller A., Fleming A.J. & Smart C.C. (2002) The ABC transporter SpTUR2 confers resistance to the antifungal diterpene sclareol. *The Plant Journal* **30**, 649–662.
van den Brule S. & Smart C.C. (2002) The plant PDR family of ABC transporters. *Planta* **216**, 95–9106.
Wagner G.J. (1991) Secreting glandular trichomes, more than just hairs. *Plant Physiology* **96**, 675–679.
Wagner G.J., Wang E. & Shepherd R.W. (2004) New approaches for studying and exploiting an old protuberance, the plant trichome. *Annals of Botany* **93**, 3–11.
Walker J.E., Saraste M., Runswick M.J. & Gay N.J. (1982) Distantly related sequences in the alpha- and beta-subunits of ATP synthase, myosin, kinases and other ATP-requiring enzymes and a common nucleotide binding fold. *EMBO Journal* **1**, 945–951.
Wang E.M. & Wagner G.J. (2003) Elucidation of the functions of genes central to diterpene metabolism in tobacco trichomes using posttranscriptional gene silencing. *Planta* **216**, 686–691.
Wang E.M., Wang R., DeParasis J., Loughrin J.H., Gan S.S. & Wagner G.J. (2001) Suppression of a P450 hydroxylase gene in plant trichome glands enhances natural-product-based aphid resistance. *Nature Biotechnology* **19**, 371–374.
Weinhold A. & Baldwin I.T. (2011) Trichome-derived O-acyl sugars are a first meal for caterpillars that tags them for predation. *Proceedings of the National Academy of Sciences of the United States of America* **108**, 7855–7859.
Wesley S.V., Helliwell C.A., Smith N.A., Wang M.B., Rouse D.T., Liu Q., … Waterhouse P.M. (2001) Construct design for efficient, effective and high-throughput gene silencing in plants. *The Plant Journal* **27**, 581–590.
Wittenburg H. & Carey M.C. (2002) Biliary cholesterol secretion by the twinned sterol half-transporters ABCG5 and ABCG8. *The Journal of Clinical Investigation* **110**, 605–609.
Xi J., Xu P. & Xiang C.-B. (2011) Loss of AtPDR11, a plasma membrane-localized ABC transporter, confers paraquat tolerance in *Arabidopsis thaliana*. *The Plant Journal* **69**, 782–791.
Yazaki K. (2006) ABC transporters involved in the transport of plant secondary metabolites. *FEBS Letters* **580**, 1183–1191.
Zerback R., Bokel M., Geiger H. & Hess D. (1989) A kaempferol 3-glucosylgalactoside and further flavonoids from pollen of *Petunia hybrida*. *Phytochemistry* **28**, 897–899.

Received 3 February 2016; accepted for publication 29 August 2016

SUPPORTING INFORMATION

Additional Supporting Information may be found in the online version of this article at the publisher's web-site:

Supplemental Figure 1. *PDR* expression profile of petunia leaves and trichomes.
Supplemental Figure 2. PhPDR phylogeny in comparison to other species.
Supplemental Figure 3. Predicted structure of PDR2.
Supplemental Figure 4. Transcriptional responses of *PhPDR2*.
Supplemental Figure 5. Sclareol assays.
Supplemental Figure 6. Petuniasterone MS/MS studies.
Supplemental Figure 7. Absolute petuniolide and petuniasterone levels in leaves and leaf margins of wild type and *pdr2* plants.
Supplemental Table 1. Structure and amount of selected petuniasterone, petuniolide and flavonoid derivatives found in *pdr2* and wild-type lines.
Supplemental Table 2. XCMS analysis of content reduction of unknowns metabolites in *pdr*2 lines.
Supplemental table 3. Metabolites and EICs for quantification of leaf and leaf margin petunioides and petuniasterones and the standard corticosterone.